DOI: 10.1002/chem.200601368

Shape-Controlled Synthesis and Self-Assembly of Hexagonal Covellite (CuS) Nanoplatelets

Weimin Du, Xuefeng Qian,* Xiaodong Ma, Qiang Gong, Hongliang Cao, and Jie Yin[a]

Abstract: Single-crystalline, hexagonal covellite (CuS) nanoplatelets were successfully synthesized through a facile, inexpensive, reproducible, and improved solvothermal process in toluene at 120 °C for 24 h with hexadecylamine as a capping agent and copper acetate and carbon disulfide as precursors. These nanoplatelets are about 26 ± 1.5 nm in diameter and 8 ± 1.2 nm thick, and have a tendency to self-assemble into pillarlike nanostructures with face-to-face stacks, raftlike nanostructures with side-by-side arrays, and stratiform nanostructures with layer-by-layer self-assembly. The crystal shape, morphology, and crystallographic orientation of the covellite obtained were investigated by means of XRD, TEM, and high-resolution TEM, and a potential self-assembly mechanism was proposed.

Keywords: covellite · crystal growth · metal sulfides · nanoplatelets · self-assembly

Introduction

The controlled synthesis of nanomaterials has attracted much attention, not only as a result of their fundamental shape- and size-dependent properties and important technological applications, but also for their self-assembling potential for use in devices.[1] Furthermore, precise control of their chemical composition, crystal structure, size, shape, and surface chemistry allows one to observe the unique properties of nanocrystals, and to tune their chemical and physical properties as desired.[2] Since the solution-phase synthetic approach in organic solvents was first proposed by Steigerwald et al., and systematically developed by Brus et al. to prepare a variety of nanoscale II-VI and III-V semiconductors in the mid-1980s to mid-1990s,[3a–c] a series of highly monodisperse nanomaterials, for example, CdS, CdSe, CdTe, ZnS, PbS, and MnS, have been prepared by using an organometallic approach and alternative approaches in diverse surfactant or solvent systems, in which single precursors, multiple precursors, or simple inorganic precursors were used. Aside from the work by Murray et al. for the growth of CdSe nanocrystals in trioctylphosphane oxide (TOPO),[3d] other scientific groups, such as those of Alivisatos, Korgel, Cheon, Hyeon, and Peng,[3e–i] have also achieved many outstanding results in the controlled synthesis of various nanomaterials. With the development of synthetic technologies, other interesting and general routes were also developed to prepare monodisperse or uniformly shaped nanocrystals, which include liquid–solid–solution (LSS) phase transfer synthetic routes, solvent-free thermolysis of metal thiolate precursors, rapid microwave-assisted methodologies, and so forth.[4] Though great progress has been made in preparing controlled nanocrystals and understanding the mechanism of their formation, the toxicity and the difficulty in preparing organometallic precursors has limited their popularity. The requirements for relatively high temperatures or a more complicated operational process has made the experimental process difficult. Therefore, it still remains a challenge to explore a simple and general strategy to synthesize monodisperse nanomaterials with controlled shapes for different systems.

The self-assembly of uniform nanoparticles into well-defined two- or three-dimensional superstructures has recently attracted rapidly growing interest owing to their important applications in nanoelectronics, magnetics, optoelectronics, photonics, heterogeneous catalysis, and so forth.[5] For the self-assembly of nanoparticles, organic capping reagents usually play critical roles in reducing the activity of the nanocrystals (building blocks) to promote or tune the ordered self-assembly.[6] Relative to the isotropic hexagonal self-assembly of spherical or near-spherical nanoparticles, the self-

[a] Dr. W. Du, Prof. X. Qian, Dr. X. Ma, Dr. Q. Gong, Dr. H. Cao, Prof. J. Yin
School of Chemistry and Chemical Technology
Shanghai Jiao Tong University
Shanghai 200240 (P.R. China)
Fax: (+87) 21-5474-1297
E-mail: xfqian@sjtu.edu.cn

Supporting information for this article is available on the WWW under http://www.chemeurj.org/ or from the author.

assembly of anisotropic nanostructures, such as nanorods, nanowires, nanodisks, and nanotubes, requires more effort. Fortunately, some powerful pathways have been developed for manipulating building blocks into more complex self-assembling superstructures, either from bottom-up techniques (by means of self-assembly in solution) or from top-down techniques (by using different lithographic methods).[7] For example, self-assemblies based on nanoplatelet or nanodisk building blocks have been fabricated recently, which include CuS, Cu_2S nanodisks;[3h,4b] hexagonal close-packed Co nanodisks; silver nanoplates; Bi_2Te_3 hexagonal nanoplatelets; and LaF_3 triangular nanoplates and nanodisks.[8] Different self-assembly mechanisms were suggested, for example, Co and LaF_3 nanodisks self-assemble owing to their physical or structural properties;[8a,e] the T- and L-shaped junctions of CuS nanodisks self-assemble as a result of van der Waals attractions, packing entropy, and polar interparticle interactions;[3h] the self-assembly of Bi_2Te_3 nanoplatelets that pack along the *c* axis in a top–bottom–top–bottom arrangement results in a reduction in lattice energy mismatch;[8c] and the long-range one- and three-dimensional arrays of Cu_2S nanodisks self-assemble owing to van der Waals attractions and the individual nanocrystal dipole–dipole moments aligning with respect to one another.[4b] Though different mechanisms for various systems have been proposed, further investigations into self-assembly phenomena will largely enrich our understanding of the nanoworld.

In this paper, covellite (CuS) was chosen because it is an important semiconductor that shows metallic conductivity, transforms into a superconductor at 1.6 K,[9a] and exhibits fast-ion conduction at high temperatures.[9b] Furthermore, it also has potential application as a thermoelectric cooling material, an optical filter, an optical recording material, a solar cell, and a superionic material.[9c–e] Though several methods have been developed to prepare CuS, such as hydrothermal, γ-radiation, microemulsion, or sonochemical techniques, [10] products with spherical or irregular shapes, or conglomerates with a large size distribution were obtained, apart from when a metal compound solvated by dichlorobenzene was used as the precursor at relatively high temperature.[3h] Therefore, the development of "soft chemistry" methods that are suitable for the synthesis of covellite with controlled shape and size, in a simple way, or with simple precursors, still remains a major challenge. An improved solvothermal method in toluene was utilized in the present work for the shape-controlled synthesis of single-crystalline hexagonal CuS nanoplatelets. In addition, these nanoplatelets can self-assemble into pillarlike, raftlike, and stratiform nanostructures by tuning the reaction parameters. This approach proved to be a facile, inexpensive, and reproducible method that can be extended to other systems.

Results and Discussion

Morphology, structural characterization, and crystallographic orientation analysis of hexagonal CuS nanoplatelets: CuS nanoplatelets were synthesized by using the improved solvothermal process in toluene with hexadecylamine (HDA) as the capping agent. The detailed reaction conditions are listed in Table 1. When the reaction was carried out at 120 °C for 24 h, the as-prepared CuS nanocrystals (sample 1 in Table 1) had a strong self-assembling tendency, and at first glance, one-dimensional superstructures were formed by the array of CuS nanorods (Figure 1). However, careful observation reveals that the building blocks of the one-dimensional superstructures are, in fact, the hexagonal nanoplatelets of CuS.

Table 1. Detailed experimental conditions and the corresponding results of CuS nanocrystals.[a]

Sample	Figure no.	$Cu(Ac)_2{\cdot}H_2O$ [mmol]	HDA [mmol]	CS_2 [ml]	*T* [°C]	*t* [h]	Morphology
1	1A–C, 3, 4, 5C	0.5	3	1	120	24	hexagonal nanoplatelets with pillarlike, raftlike nanostructures
2	5A	0.5	3	1	120	2	monodisperse platelike nanocrystals
3	5B	0.5	3	1	120	6	similar to sample 2
4	5D	0.5	3	1	120	48	hexagonal nanoplatelets with stratiform nanostructure
5	7	0.5	3	0.015	120	24	similar to sample 2
6	S3A[b]	0.5	3	1	150	24	aggregated nanocrystals
7	S3B[b]	0.5	3	1	180	24	aggregated nanocrystals
8	–	0.5	2	1	120	24	similar to sample 1
9	–	0.5	5	1	120	24	similar to sample 1

[a] A typical experiment (sample 1) refers to a solution of copper acetate (0.5 mmol), HDA (3 mmol), and CS_2 (1 mL) in toluene (39 mL), which was treated at 120 °C for 24 h. [b] See the Supporting Information.

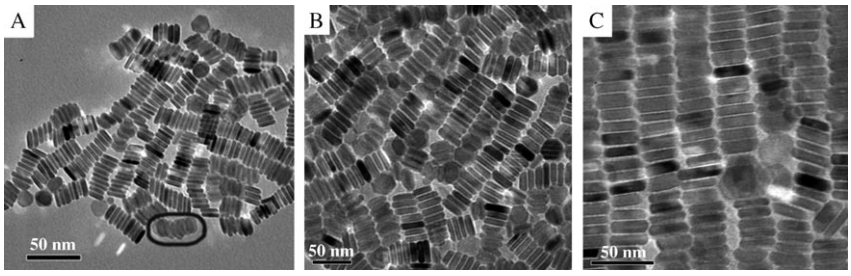

Figure 1. TEM images (at different magnifications) of typical CuS nanoplatelets synthesized at 120 °C for 24 h (sample 1 in Table 1).

The circled area in Figure 1A clearly shows that the one-dimensional CuS superstructures are composed of hexagonal nanoplatelets that are stacked face-to-face and are tilted by a certain angle because if the nanocrystals were not tilted then they would look like cylindrical rods (see Figure S1 in the Supporting Information). Some discrete nanoplatelets that lie flat on the substrate or are tilted by certain angles (Figure 1A and B) also confirmed that the building blocks were hexagonal nanoplatelets. The size of the CuS hexagonal nanoplatelet was calculated from Figure 1C to be about 26 ± 1.5 nm in diameter and 8 ± 1.2 nm thick. The space between the face-to-face stacked nanoplatelets is about 1.8 nm, which is somewhat less than the length of $C_{16}NH_2$, which is calculated to be 2.28 nm according to the formula L (nm) $=0.25+0.127n$ (in which n is the number of carbon atoms in the alkyl chain).[11] This result implies that the hexagonal nanoplatelets were capped by a layer of fatty amines (which can be confirmed by the IR spectrum shown in Figure S2 in the Supporting Information), which interpenetrate neighboring fatty amines on a nanoplatelet surface.[12] Further observation revealed that some raftlike nanostructures (two-dimensional structures) assembled by means of edge-to-edge stacking of CuS nanopillars were also formed beside pillars of CuS nanoplatelets (Figure 1C).

The X-ray powder-diffraction pattern and high-resolution TEM (HRTEM) images were used to determine the crystal phase and the shape of the products obtained. The XRD pattern (Figure 2A) shows that all the diffraction peaks can be indexed to the hexagonal phase of the covellite structure (JCPDS no. 6-464) with the $P6_3/mmc$ space group and a primitive hexagonal unit cell with $a=3.792$ and $c=16.344$ Å. No other impurities, such as $Cu_{1.8}S$, Cu_7S_4, $Cu_{1.96}S$, Cu_2S, oxides, or organic compounds related to the reactants, were detected. Other samples prepared in this work presented similar profiles. Differences in the diffraction peaks were observed when compared with the standard pattern. For example, the intensities of the 103 peak and the 006 peak are lower than those of the standard pattern, and both of them are broadened and overlap with each other. This difference implies that the growth of certain crystal facets is restrained and a special morphology is obtained. Furthermore, the intensity of the 110 peak in the XRD pattern is particularly strong, which indicates the preferential growth orientation of the hexagonal CuS nanoplatelets. On the other hand, the Balls and Sticks software package helps to illustrate the relationship between the crystallographic orientation and the favored growth direction of CuS nanoplatelets.[4b] It is well known that the covellite crystal contains two types of inequivalent sites for Cu and S. One third of the Cu atoms are coordinated to three S atoms in a triangle, whereas the remaining Cu atoms are surrounded by four S atoms to form a tetrahedron, in which the spatial location of the Cu and S atoms (Cu^1 at 0.333, 0.667, 0.75; Cu^2 at 0.333, 0.667, 0.107; S^1 at 0.333, 0.667, 0.25; S^2 at 0, 0, 0.064) were determined by simulating the XRD pattern of bulk covellite.[13] From a supercell model of CuS in which $A=3a$, $B=3b$, and $C=c$ (Figure 2B), it was found that the CuS crystal consists of alternating CuS_3–Cu_3S–CuS_3 layers and S–S layers along the z axis (c axis). Furthermore, the interactions within the CuS_3–Cu_3S–CuS_3 layers are covalent bonds, whereas the interactions between the S–S layers are van der Waals forces.[9a,14a,b] A similar layered or pseudographitic structure is also exhibited by several III-VI members of the GaS family.[14c] When considering the spatial structure of CuS, it is reasonable to believe that the intrinsic anisotropic characteristics of CuS might dominate the shape of the primary CuS particles (i.e., platelet seed), and further affect the growth rate of the crystal along the top–bottom crystalline planes and along the c axis because the crystal facets tend to develop on the low-index planes to minimize the surface energy during the growth of the crystal. On the other hand, modification of HDA on the surfaces of the CuS nanocrystals may increase the energy difference between the top and bottom facets and the side facets.

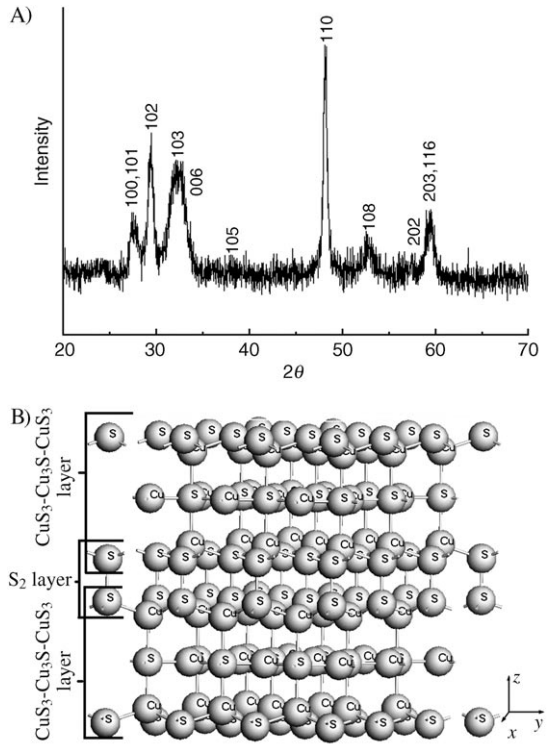

Figure 2. A) The XRD pattern of a typical copper sulfide sample. B) The spatial structure of the covellite supercell with dimensions of $A=3a$, $B=3b$, and $C=c$.

To gain further insights into the crystallographic orientation of the CuS nanoplatelets, the two kinds of primary nanoplatelets found on the substrate, either standing on their edge in stacked pillars of nanoplatelets or lying flat on the substrate, were studied by using HRTEM images. Lattice images of the platelets in different orientations reveal that the nanoplatelets are single crystals with the $<001>$ direction oriented in the direction of the short axis. The HRTEM image of a hexagonal nanoplatelet lying flat on its hexagonal facet (Figure 3A) clearly shows that the 3.29 and

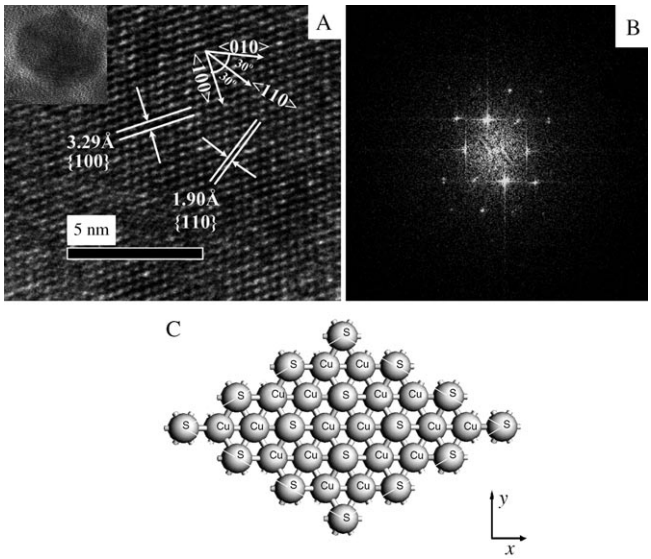

Figure 3. A) HRTEM image of a hexagonal nanoplatelet lying flat on the substrate with the incident electron beam from the $<001>$ direction; the inset shows an overall HRTEM picture of the hexagonal CuS nanoplatelet. B) The corresponding fast Fourier transform (FFT) pattern of the hexagonal nanoplatelet shown in A. C) Corresponding crystallographic model of the CuS covellite structure viewed from the same direction as the imaged nanocrystal.

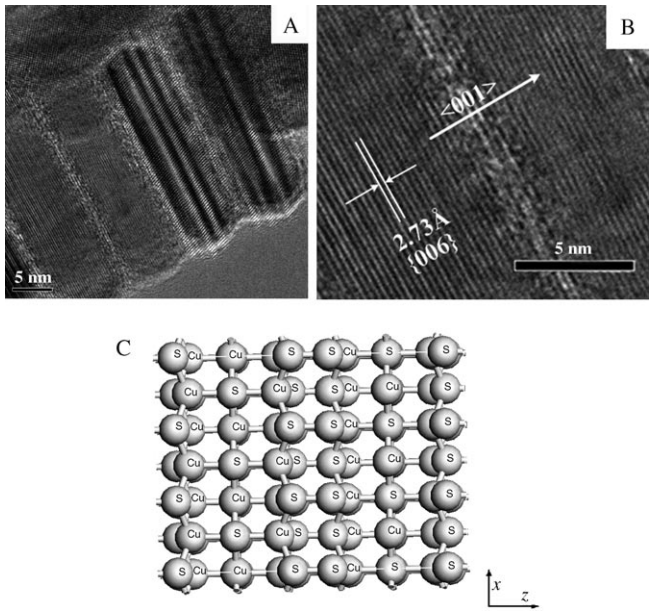

Figure 4. A) HRTEM image of several hexagonal nanoplatelets standing edge-on perpendicular to the substrate with the electron beam incident in the $<010>$ direction. B) High magnification image of A. C) Corresponding crystallographic model of the hexagonal CuS structure viewed from the same direction as the imaged nanocrystal.

1.90 Å lattice spacings correspond to the {100} and {110} *d* spacing, respectively, of hexagonal CuS (covellite) and an angle of 30° between $<100>$ (or $<010>$) and $<110>$ is consistent with the hexagonal crystal structure of covellite CuS. The ordered hexagonal-like spot arrays (Figure 3B), shown by the fast Fourier transform spectrum (FFT), confirm that hexagonal structures of CuS nanoplatelets are formed. The HRTEM image (Figure 4B) shows a lattice spacing of 2.73 Å, which is consistent with {006} *d* spacing of hexagonal CuS (covellite) and indicates that hexagonal CuS nanoplatelets preferentially stack along the hexagonal facet, namely, the $<001>$ direction, rather than the side facet (Figure 4A). When the nanoplatelets aligned in an edge-on manner, modulated fringes appeared owing to double diffraction, which is caused by stacking faults, as shown in Figure 4A. Similar phenomena have been observed in Au nanorods and Ag nanowires that are twinned along their lengths.[15] The atomic models in Figures 3C and 4C show that the arrangement of Cu and S atoms viewed from the $<001>$ and $<010>$ directions, respectively, are consistent with the HRTEM images because the nanoplatelet morphology obtained reflects the internal hexagonal CuS crystal structure. All of these results reveal that the nanoplatelets are single-crystalline structures and the $<001>$ direction is the slowest growth direction. Therefore, it is reasonable to believe that the formation of CuS nanoplatelets with hexagonal morphology results from accelerating the growth of six energetically equivalent high-index crystalline planes {110}.

Formation and self-assembly mechanism of hexagonal nanoplatelets: Further experiments showed that the size and self-assembly of CuS platelets can be tuned simply by changing the reaction time. When the reaction time was 2 h, almost monodisperse plateletlike particles with a diameter of about 7 ± 3 nm were obtained (Figure 5A). After the reaction was carried out for 6 h, monodisperse CuS nanoplatelets were still the exclusive products (Figure 5B), except that the diameter was increased to 12 ± 1.5 nm owing to the famous Ostwald ripening process. Closer observation

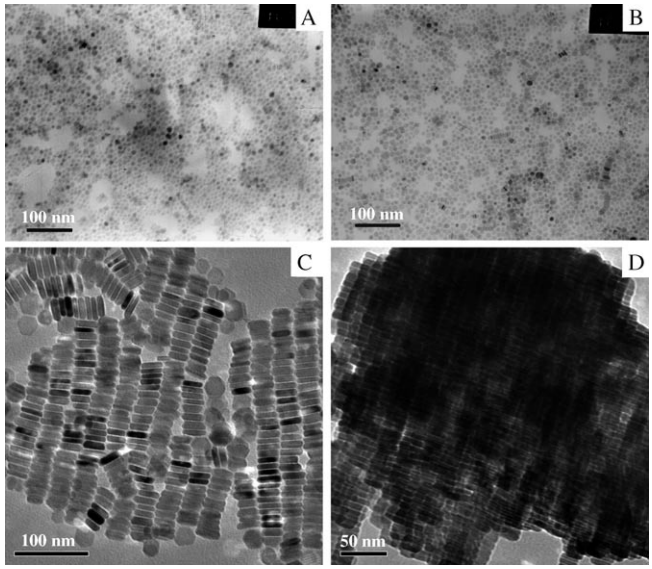

Figure 5. TEM images of CuS nanoplatelets formed at different reaction times while all other reaction parameters remain unchanged: A) 2 h (sample 2), B) 6 h (sample 3), C) 24 h (sample 1), and D) 48 h (sample 4).

showed that a few arrays had started to appear, although the surface area of the CuS nanoplatelet was still relatively small. When the reaction time was increased to 24 h, the hexagonal CuS nanoplatelets formed with larger top–bottom surface areas and tended to stack together to form extended nanopillars (Figure 5C). These nanoplatelets are about 26 ± 1.5 nm in diameter and 8 ± 1.2 nm thick, as previously described. When the reaction time was increased to 48 h, these CuS nanopillars evolved into stratiform nanostructures with layer-by-layer self-assembly in the same direction. Because the stratiform nanostructures were comprised of several layers of raftlike nanostructures, a darker TEM image was obtained owing to the difficulty of the electron beam penetrating the sample (Figure 5D). Based on the above experiments, it is reasonable to believe that the intrinsic anisotropic structure of CuS, the capping ligand (HDA), and van der Waals attraction, have cooperative effects on the formation and self-assembly of the hexagonal CuS nanoplatelets. The whole process is illustrated in Figure 6.

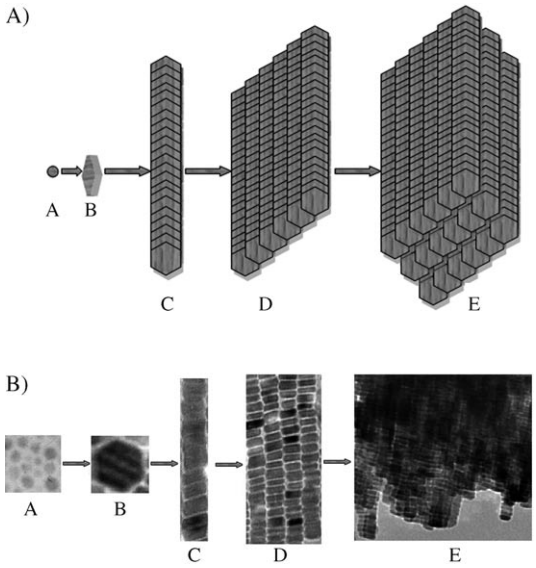

Figure 6. A) Schematic illustration of the self-assembly of CuS hexagonal nanoplatelets into pillarlike, raftlike, and stratiform nanostructures. For the sake of clarity, the HDA surfactant was omitted. B) TEM images corresponding to the schematic representation.

As mentioned in the above discussion, the anisotropic structure is beneficial for the formation of platelike CuS. Furthermore, it is generally believed that materials with hexagonal crystal structures are particularly predisposed to anisotropic growth, as the {001} planes exhibit different surface energies relative to the {100} and {110} crystal planes.[4b] Therefore, the amine may preferentially bind to the {006} facets and inhibit growth in the $<001>$ direction after the nucleus has formed, in the same way as Co nanoplatelets that are prepared in the presence of an amine capping ligand[8a] owing to the different surface energies of the CuS hexagonal crystal structure. (Detailed FTIR spectra of typical CuS nanoplatelets are presented in Figure S2 in the Supporting Information.) The previous calculation also indicated that the fatty chains of HDA that cap the CuS surface were intertwisted, which might facilitate the controlled conglomeration of hexagonal CuS nanoplatelets. Meanwhile, the van der Waals forces between the hexagonal CuS nanoplatelets capped by amines are greater for nanoplatelets oriented in a face-to-face way compared with nanoplatelets oriented in an edge-to-edge way as a result of the much greater interfacial contact area provided by its platelike shape.[3h] This packing mode can maximize the entropy of the self-assembled structure by minimizing the excluded volume per nanoplatelet in the array through the existence of a nematic phase, which was first suggested by Onsager,[16a] confirmed by Frenkel and Eppenga by means of computer simulations,[16b] and demonstrated experimentally by Lekkerkerker and co-workers.[16c] Therefore, it is believed that the preferential array of CuS nanoplatelets through the [006] planes resulted in the formation of a pillarlike nanostructure through a face-to-face stack along the $<001>$ direction. With longer reaction times, the lateral surface areas were gradually enlarged and the interactions between nanopillars were increased owing to the increase in length of the nanopillars, which resulted in the edge-to-edge array. In some ways, these interactions among nanopillars are similar to those of the arrays of nanorods, for example, higher lateral capillary forces, van der Waals attractions, and a screened Coulomb repulsion between nanorods.[7b] As a result, raftlike nanostructures were formed by edge-to-edge arrays of nanopillars. Given sufficient reaction times, these edge-to-edge arrays might extend into two-dimensional planes, and self-assemble into a stratiform nanostructure through layer-by-layer stacking in a three-dimensional way (shown in Figure 5D).

Effects of reaction parameters on the morphologies of CuS: To study the influences of other reaction parameters on the morphologies of CuS, experiments were designed to vary these parameters, for example, the amount of CS_2, the reaction temperature, and so forth. When the amount of carbon disulfide was 0.015 mL (to ensure there is no excess sulfur in the reaction mixture), the CuS that was obtained was still plateletlike, but smaller in size and with a wider size distribution (from 4 to 15 nm) (Figure 7). This result implied that the excess of carbon disulfide could enhance the exchange rate between the growing nanocrystals and the

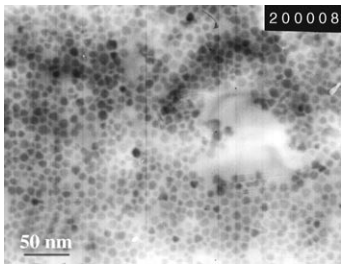

Figure 7. TEM image of sample 5 prepared with CS_2 (0.015 mL) (Cu/S = 1:1 molar ratio) while all other reaction parameters remain unchanged.

monomer reservoir, which is beneficial for the control of the size and the shape. In addition, if the reaction was carried out at higher temperatures, such as 150 or 180 °C, for 24 h (samples 6 and 7 in Table 1, respectively), then large aggregates of CuS were obtained owing to uncontrolled growth (see Figure S3 in the Supporting Information). On the other hand, it is known that the coordination number between the copper ion and the amino group is 4, so the minimum amount of HDA was defined as 2 mmol. When the amount of HDA was changed from 2 to 5 mmol, the shape and the size distribution of the hexagonal nanoplatelets were almost unchanged.

Conclusion

In summary, hexagonal CuS nanoplatelets were successfully synthesized by means of the improved solvothermal method in toluene by using HDA as the capping ligand. These hexagonal nanoplatelets are single crystals and hexagonal in shape with the *c* axis oriented perpendicular to the faster growing {110} planes. Hexagonal nanoplatelet growth is limited to the $<001>$ direction and predominantly occurs along the six energetically equivalent $<110>$ directions. These hexagonal nanoplatelets can self-assemble into pillarlike, raftlike, and stratiform nanostructures (with only a few stacking defects) as a result of van der Waals attractions and the mechanism of the packing entropy. Their high quality should be more valuable for further theoretical and practical explorations of their shape- and size-dependent properties, and their intriguing self-assembly capability enables them to serve as novel nano building blocks for new nanodevice applications. Furthermore, this method also opens a new way for shape- and size-controlled synthesis of other semiconductor metal sulfides.

Experimental Section

Materials: Copper acetate monohydrate, carbon disulfide, and toluene were analytical grade reagents (Shanghai Chemical Reagent). HDA (92% mass fraction) was purchased from Merck-Schuchardt. All reagents were used as received without further purification.

Synthesis: In a typical process to prepare sample 1, copper acetate monohydrate (0.5 mmol) and HDA (3 mmol) were dissolved in toluene (39 mL) at room temperature to give a homogeneous and clear blue solution after the resulting mixture was heated to 60 °C and maintained for 30 min. The resulting solution was then transferred to a 50 mL Teflon-lined stainless steel autoclave before carbon disulfide (1 mL) was added. After the autoclave was sealed and maintained at 120 °C for 24 h in a preheated oven, it was removed and cooled to about 60 °C to yield CuS after it was treated with excessive ethanol and dried in a vacuum oven. The products obtained can be easily dispersed in organic solvents, such as toluene and chloroform.

Characterization: The crystal phase of the as-prepared products was characterized by using a Rigaku D/Max-3C diffractometer equipped with a rotating anode and a $Cu_{K\alpha}$ radiation source ($\lambda = 0.15418$ nm), with 2θ from 20 to 80° at a scanning rate of 6° min^{-1}. The X-ray tube voltage and current were set at 40 kV and 20 mA, respectively. The morphologies and structural analyses of the samples were carried out by means of TEM (JEOL JEM-100CXII, with an accelerating voltage of 100 kV; JEOL JEM-2010, with an accelerating voltage of 200 kV) and HRTEM (JEOL, JEM-2100F, with an accelerating voltage of 200 kV). FTIR spectra were recorded by using a Perkin–Elmer Paragon 1000 FTIR spectrometer.

Acknowledgement

The work described in this paper was supported by the National Science Foundation of China (no. 20671061). We thank the Analysis and Testing Center of Shanghai Jiao Tong University for their kind help with HRTEM measurements.

[1] a) C. B. Burda, X. B. Chen, R. Narayanan, M. A. El-Sayed, *Chem. Rev.* **2005**, *105*, 1025; b) Y. N. Xia, P. D. Yang, Y. G. Sun, Y. Y. Wu, B. Mayers, B. Gates, Y. D. Yin, F. Kim, H. Q. Yan, *Adv. Mater.* **2003**, *15*, 353; c) N. Tessler, V. Medvedev, M. Kazes, S. Kan, U. Banin, *Science* **2002**, *295*, 1506.

[2] a) Y. D. Yin, A. P. Alivisatos, *Nature* **2005**, *437*, 664; b) A. P. Alivisatos, *Science* **1996**, *271*, 933; c) S. Sun, C. B. Murray, D. Weller, L. Folks, A. Moser, *Science* **2000**, *287*, 1989.

[3] a) M. L. Steigerwald, C. R. Sprinkle, *Organometallics* **1988**, *7*, 245; b) J. G. Brennan, T. Siegrist, P. J. Carroll, S. M. Stuczynski, L. E. Brus, M. L. Steigerwald, *J. Am. Chem. Soc.* **1989**, *111*, 4141; c) J. G. Brennan, T. Siegrist, P. J. Carroll, S. M. Stuczynski, P. Reynders, L. E. Brus, M. L. Steigerwald, *Chem. Mater.* **1990**, *2*, 403; d) C. B. Murray, D. J. Norris, M. G. Bawendi, *J. Am. Chem. Soc.* **1993**, *115*, 8706; e) L. Manna, E. C. Scher, A. P. Alivisatos, *J. Am. Chem. Soc.* **2000**, *122*, 12700; f) Y. W. Jun, J. H. Lee, J. S. Choi, J. W. Cheon, *J. Phys. Chem. B* **2005**, *109*, 14795; g) J. Joo, H. B. Na, T. Yu, J. H. Yu, Y. W. Kim, F. Wu, J. Z. Zhang, T. Hyeon, *J. Am. Chem. Soc.* **2003**, *125*, 11100; h) A Ghezelbash, B. A. Korgel, *Langmuir* **2005**, *21*, 9451; i) W. W. Yu, X. G. Peng, *Angew. Chem.* **2002**, *114*, 2474; *Angew. Chem. Int. Ed.* **2002**, *41*, 2368.

[4] a) X. Wang, J. Zhuang, Q. Peng, Y. D. Li, *Nature* **2005**, *437*, 121; b) M. B. Sigman, A. Ghezelbash, T. Hanrath, A. E. Saunders, F. Lee, B. A. Korgel, *J. Am. Chem. Soc.* **2003**, *125*, 16050; c) A. B. Panda, G. Glaspell, M. S. El-Shall, *J. Am. Chem. Soc.* **2006**, *128*, 2790.

[5] a) E. V. Shevchenko, D. V. Talapin, C. B. Murray, S. O'Brien, *J. Am. Chem. Soc.* **2006**, *128*, 3620; b) P. Michler, A. Imamoglu, M. D. Mason, P. J. Carson, G. F. Strouse, S. K. Buratto, *Nature* **2000**, *406*, 968; c) W. C. Chan, W. S. Nie, *Science* **1998**, *281*, 2016.

[6] a) C. B. Murray, C. R. Kagan, M. G. Bawendi, *Annu. Rev. Mater. Sci.* **2000**, *30*, 545; b) C. B. Murray, C. R. Kagan, M. G. Bawendi, *Science* **1995**, *270*, 1335; c) A. van Blaarderen, R. Ruel, P. Wiltzius, *Nature* **1997**, *385*, 321.

[7] a) M. Li, H. Schnablegger, S. Mann, *Nature* **1999**, *402*, 393; b) B. Nikoobakht, Z. L. Wang, M. A. El-Sayed, *J. Phys. Chem. B* **2000**, *104*, 8635; c) S. W. Chung, G. Markovich, J. R. Heath, *J. Phys. Chem. B* **1998**, *102*, 6685; d) F. Kim, S. Kwan, J. Akana, P. Yang, *J. Am. Chem. Soc.* **2001**, *123*, 4360; e) S. Kwan, F. Kim, J. Akana, P. Yang, *Chem. Commun.* **2001**, 447; f) Y. Huang, X. F. Duan, Q. Q. Wei, C. M. Lieber, *Science* **2001**, *291*, 630.

[8] a) V. F. Puntes, D. Zanchet, C. K. Erdonmez, A. P. Alivisatos, *J. Am. Chem. Soc.* **2002**, *124*, 12874; b) S. H. Chen, D. L. Carroll, *J. Phys. Chem. B* **2004**, *108*, 5500; c) W. G. Lu, Y. Ding, Y. X. Chen, Z. L. Wang, J. Y. Fang, *J. Am. Chem. Soc.* **2005**, *127*, 10112; d) Y. W. Zhang, X. Sun, R. Si, L. P. You, C. H. Yan, *J. Am. Chem. Soc.* **2005**, *127*, 3260; e) Y. Cheng, Y. S. Wang, Y. H. Zheng, Y. Qin, *J. Phys. Chem. B* **2005**, *109*, 11548.

[9] a) W. Liang, M. H. Whangbo, *Solid State Commun.* **1993**, *85*, 405; b) M. T. S. Nair, P. K. Nair, *Semicond. Sci. Technol.* **1989**, *4*, 191; c) T. Chivers, *J. Chem. Soc., Dalton Trans.* **1996**, 1185; d) H. Toyoji, H. Yao, *Jpn. Kokai Tokyo Koho* **2002**, *173*, 622; e) F. Mongellaz, A. Fillot, J. De Lallee, *Proc. SPIE-Int. Soc. Opt. Eng.* **1994**, *156*, 2227.

[10] a) X. Y. Chen, Z. H. Wang, X. Wang, R. Zhang, X. Y. Liu, W. J. Lin, Y. T. Qian, *J. Cryst. Growth* **2004**, *263*, 570; b) Z. P. Qiao, Y. Xie, J. G. Xu, Y. J. Zhu, Y. T. Qian, *J. Colloid Interface Sci.* **1999**, *214*, 459; c) L. Gao, E. B. Wang, S. Y. Lian, Z. H. Kang, Y. Lan, D. Wu, *Solid State Commun.* **2004**, *130*, 309; d) H. Wang, J. R. Zhang, X. N. Zhao, S. Xu, J. J. Zhu, *Mater. Lett.* **2002**, *55*, 253.

[11] C. D. Bain, J. Evall, G. M. Whitesides, *J. Am. Chem. Soc.* **1989**, *111*, 7155.

[12] A. Badia, W. Gao, S. Singh, L. Demers, L. Cuccia, L. Reven, *Langmuir* **1996**, *12*, 1262.

[13] L. G. Berry, *Am. Mineral.* **1954**, *39*, 504.

[14] a) R. A. D. Pattrick, J. F. W. Mosselmans, J. M. Charnock, K. E. R. England, G. R. Helz, C. D. Garner, D. J. Vaughan, *Geochim. Cosmochim. Acta* **1997**, *61*, 2023; b) G. W. Luther, S. Theberge, T. Rozan, D. Rickard, C. C. Rowlands, A. Oldroyd, *Environ. Sci. Technol.* **2002**, *36*, 394; c) J. A. Hollingsworth, D. M. Poojary, A. Clearfield, W. E. Buhro, *J. Am. Chem. Soc.* **2000**, *122*, 3562.

[15] a) H. Chen, Y. Gao, H. Zhang, L. Liu, H. Yu, H. Tian, S. Xie, J. Li, *J. Phys. Chem. B* **2004**, *108*, 12038; b) C. J. Johnson, E. Dujardin, S. A. Davis, C. J. Murphy, S. Mann, *J. Mater. Chem.* **2002**, *12*, 1765; c) Y. Sun, B. Mayers, T. Herricks, Y. Xia, *Nano Lett.* **2003**, *3*, 955.

[16] a) L. Onsager, *Phys. Rev.* **1942**, *62*, 558; b) D. Frenkel, R. Eppenga, *Phys. Rev. Lett.* **1982**, *49*, 1089; c) F. M. van der Kooij, H. N. W. Lekkerkerker, *J. Phys. Chem. B* **1998**, *102*, 7829.

Received: September 23, 2006
Published online: January 2, 2007

